THE JOURNAL OF BIOLOGICAL CHEMISTRY VOL. 286, NO. 48, pp. 41530–41538, December 2, 2011

Ubiquitin Ligase Substrate Identification through Quantitative Proteomics at Both the Protein and Peptide Levels[S]

Received for publication, April 7, 2011, and in revised form, October 7, 2011 Published, JBC Papers in Press, October 10, 2011, DOI 10.1074/jbc.M111.248856

Kimberly A. Lee[‡], Lisa P. Hammerle[§], Paul S. Andrews[¶], Matthew P. Stokes[‖], Tomas Mustelin[§], Jeffrey C. Silva[‖], Roy A. Black[§], and John R. Doedens[§1]

From the Departments of [‡]Molecular Sciences and [§]Inflammation, Amgen, Seattle, Washington 98119, the [¶]Department of Lead Discovery, Amgen, Cambridge, Massachusetts 02142, and [‖]Cell Signaling Technology Inc., Danvers, Massachusetts 01923

Background: Identification of ubiquitin ligase substrates remains an unmet challenge.
Results: Two proteomic strategies were used to identify novel substrates of the E3 ligase HRD1.
Conclusion: These methods identified populations of substrates enriched for potential targets of endoplasmic reticulum-associated degradation.
Significance: This approach should be broadly useful for E3 ligase substrate identification, and the identified substrates provide insight into the role of HRD1 in disease.

Protein ubiquitination is a key regulatory process essential to life at a cellular level; significant efforts have been made to identify ubiquitinated proteins through proteomics studies, but the level of success has not reached that of heavily studied post-translational modifications, such as phosphorylation. HRD1, an E3 ubiquitin ligase, has been implicated in rheumatoid arthritis, but no disease-relevant substrates have been identified. To identify these substrates, we have taken both peptide and protein level approaches to enrich for ubiquitinated proteins in the presence and absence of HRD1. At the protein level, a two-step strategy was taken using cells expressing His_6-tagged ubiquitin, enriching proteins first based on their ubiquitination and second based on the His tag with protein identification by LC-MS/MS. Application of this method resulted in identification and quantification of more than 400 ubiquitinated proteins, a fraction of which were found to be sensitive to HRD1 and were therefore deemed candidate substrates. In a second approach, ubiquitinated peptides were enriched after tryptic digestion by peptide immunoprecipitation using an antibody specific for the diglycine-labeled internal lysine residue indicative of protein ubiquitination, with peptides and ubiquitination sites identified by LC-MS/MS. Peptide immunoprecipitation resulted in identification of over 1800 ubiquitinated peptides on over 900 proteins in each study, with several proteins emerging as sensitive to HRD1 levels. Notably, significant overlap exists between the HRD1 substrates identified by the protein-based and the peptide-based strategies, with clear cross-validation apparent both qualitatively and quantitatively, demonstrating the effectiveness of both strategies and furthering our understanding of HRD1 biology.

The 76-amino acid protein ubiquitin plays a central role in the regulation of cellular processes. In addition to targeting proteins for proteasomal degradation, ubiquitination modulates membrane protein trafficking (1), alters protein-protein interactions, and controls the activity of many signal transduction pathways (2). A large family of enzymes involved in ubiquitin conjugation controls these diverse functions.

Ubiquitin conjugation to a target protein occurs via a three-step process. First, the C terminus of ubiquitin is coupled to a ubiquitin-activating enzyme (E1) via a thioester linkage to a reactive cysteine residue on the E1. Next, the activated ubiquitin is transferred to a ubiquitin-conjugating enzyme (E2), again coupled through a thioester linkage. Finally, a complex of the E2 ubiquitin and an E3 ubiquitin ligase recognizes the substrate and catalyzes the transfer of ubiquitin to a lysine residue on the substrate, forming an isopeptide linkage between the ubiquitin C terminus and the ϵ-amino group of the lysine residue (3).

The many functions of protein ubiquitination combined with the wide range of proteins subject to this modification are reflected in the diversity of E3 ligases. Several classes of E3s exist, the largest of which is the RING domain family, with over 600 members predicted to be encoded by the human genome (4). The identification of substrates for this diverse repertoire of E3s remains a significant challenge for the field.

HRD1 (also called synoviolin) is a transmembrane RING E3 originally studied in yeast and then mammalian systems for its role in the endoplasmic reticulum-associated degradation (ERAD)[2] of misfolded membrane proteins (5–7). It was independently identified as being up-regulated in synoviocytes from rheumatoid arthritis (RA) patients (8). Transgenic mice overexpressing HRD1 developed spontaneous joint pathology characterized by synoviocyte hyperplasia and invasion into cartilage and bone, whereas heterozygous HRD1 knock-out animals showed decreased susceptibility and severity in two arthritis models (8). Both peripheral blood cells and synoviocytes from RA patients display elevated levels of HRD1 mRNA (9), and

[S] The on-line version of this article (available at http://www.jbc.org) contains supplemental Tables S1–S4 and Figs. S1–S8.

[1] To whom correspondence should be addressed: 119 NW 50th St., Seattle, WA 98107. E-mail: jdoedens@yahoo.com.

[2] The abbreviations used are: ERAD, endoplasmic reticulum-associated degradation; RA, rheumatoid arthritis; SILAC, stable isotope labeling with amino acids in cell culture; H:L, heavy to light.

HRD1 expression is up-regulated by pro-inflammatory cytokines known to contribute to RA pathogenesis (10, 11). Taken together, these findings implicate HRD1 in the pathogenesis of rheumatoid arthritis. However, disease-relevant substrates of HRD1 remain to be definitively identified.

Initial proteomic approaches to study ubiquitination primarily used yeast systems expressing tagged ubiquitin (12). Affinity reagents directed at the ubiquitin protein have also been applied (13, 14), allowing the study of native tissues without the need for exogenous protein expression, and these tactics have been combined to increase specificity for ubiquitinated proteins (15). Approaches focused on enrichment of ubiquitinated proteins are complicated by the difficulty of confirming that the identified proteins are actually ubiquitinated. High protein coverage is typically required to allow ubiquitination site identification, and targeted follow-up studies to demonstrate ubiquitination of select proteins are labor-intensive. Gel shift analysis on a proteomic scale has been proposed and applied (16), but a relatively high false positive rate is observed, and analysis may be confounded by other post-translational modifications of the observed proteins. Recently, the use of an antibody directed against the diglycine moiety left on a ubiquitinated lysine residue after trypsin digestion has been reported to enrich ubiquitinated peptides (17–20). This strategy is implicitly specific for modification with ubiquitin or a ubiquitin-like protein but has not yet been reported for the association of substrates with a particular E3 ligase.

In this study, we apply both protein level and peptide level enrichment in combination with siRNA technology and quantification by stable isotope labeling with amino acids in cell culture (SILAC) (21) to identify and validate novel HRD1 substrates.

EXPERIMENTAL PROCEDURES

Cell Lines, Antibodies, and Reagents—HeLa-TREx cells were purchased from Invitrogen and maintained in DMEM supplemented with 10% FBS, 100 units/ml penicillin, 100 μg/ml streptomycin, and 5 μg/ml blasticidin (all purchased from Invitrogen).

Stealth-Select siRNA duplexes directed against HRD1 and negative control duplexes were purchased from Invitrogen. The sense strand sequences of the siRNAs used were 5′-GGACGCCGCCAUGCUGCAGAUCAA-3′ (siRNA-1), 5′-GAGACUUGUCUGGCCUUCACCGUUU-3′ (siRNA-2), and 5′-GCCAAGAGACUGCCCUGCAACCACA-3′ (siRNA-3).

The plasmid encoding HA-ubiquitin was generated by amplifying the UBC gene from a fetal liver cDNA library (Amgen) using primers: 5′-CGG ATC CGC CAC CAT GTA CCC ATA CGA CGT TCC AGA TTA CGC TTA CCC ATA CGA CGT TCC AGA TTA CGC TAT GCA GAT CTT CGT GAA GAC-3′ (forward primer) and 5′-CGG AAT TCT TAC CCA CCT CTG AGA CGG AG-3′ (reverse primer). The resulting PCR product was digested with BamHI and EcoRI and then cloned between BamHI and EcoRI sites of pcDNA3.1 (Invitrogen). The His_6-ubiquitin plasmid was constructed by amplifying the HA-ubiquitin plasmid with primers: 5′-GCG GAT CCG CCA CCA TGC ACC ACC ATC ATC ACC ACA TGC AGA TCT TCG TGA AGA CCC-3′ (forward) and 5′-CGG AAT TCT TAC CCA CCT CTG AGA CGG AG-3′ (reverse). The resulting PCR product was digested with BamHI and EcoRI and cloned into pcDNA3.1 as above. All of the plasmid constructs were confirmed by DNA sequencing.

SILAC Labeling—HeLa-TREx cells were grown for at least six generations in SILAC DMEM (Pierce) containing 10% dialyzed FBS, and penicillin, streptomycin, and blasticidin as above. SILAC medium was supplemented with 100 mg/liter of appropriate isotopes of L-lysine and L-arginine along with 500 mg/liter L-proline to prevent conversion of arginine to proline (data not shown) (22). For experiments in which two conditions were compared, one population of cells was grown with $^{12}C_6$-lysine and $^{12}C_6$-arginine, and the other was grown with $^{13}C_6$-lysine and $^{13}C_6$-arginine. For experiments comparing three conditions, a third population of cells was grown in medium containing $^{13}C_6$,$^{15}N_2$-lysine and $^{13}C_6$,$^{15}N_4$-arginine.

Transfections—One day prior to transfection, the cells were plated to 15-cm dishes at a density of 8×10^6 cells/dish in appropriate SILAC medium lacking antibiotics. The following day, the cells were transfected with 15 μg/dish of plasmid DNA and 300 pmol/dish siRNA as appropriate using 60 μl/dish of Lipofectamine 2000 (Invitrogen) according to the manufacturer's instructions. After 4 h of incubation of the cells with liposome complexes, the transfection mixture was aspirated and replaced with fresh SILAC medium lacking antibiotics.

Treatment of Cells and Preparation of Samples for Analysis—Two days after transfection, SILAC-labeled cells were incubated with 10 μM MG132 (Calbiochem) for 4 h at 37 °C. At the end of the MG132 treatment, the medium was aspirated, and the cells were scraped into 5 ml/dish of ice-cold PBS containing 10 μM MG132. The cells were counted, and 10^8 cells of each experimental condition were pelleted for 10 min at 160 × *g* at 4 °C. The resulting cell pellets were resuspended in 5 ml of ice-cold PBS, and samples to be analyzed together were pooled and pelleted again. Cell pellets to be analyzed by peptide level enrichment were frozen on dry ice and stored at −70 °C. Aliquots of cells from each transfection condition were also reserved for analysis of HRD1 knockdown.

Aliquots of unpooled cells were resuspended in 200 μl of ice-cold buffer consisting of 50 mM Tris-HCl, pH 7.5, 150 mM NaCl, 1% Triton X-100, and one Complete-Mini EDTA-free proteinase inhibitor tablet (Roche Applied Science)/10 ml. After 30 min on ice, insoluble material was pelleted for 30 min at 13,000 × *g* in a 4 °C microcentrifuge. The resulting supernatants were transferred to fresh tubes, and the protein concentrations were determined by BCA assay (Pierce). Normalized amounts of lysate protein were separated by SDS-PAGE, and HRD1 levels were visualized on Western blots probed with a rabbit polyclonal antibody directed against the C terminus of HRD1 (Abgent) at a dilution of 1:500 followed by a donkey anti-rabbit horseradish peroxidase conjugate (Jackson Immunoresearch) diluted 1:30,000.

Cell pellets to be analyzed by protein level enrichment were resuspended in 10 ml of ice-cold lysis buffer consisting of 50 mM Tris-HCl, pH 7.5, 150 mM NaCl, 1% Triton X-100, one Complete-Mini EDTA-free proteinase inhibitor tablet, 10 μM MG132, and 1 mM iodoacetamide. After 30 min on ice, insoluble material was pelleted for 10 min at 850 × *g*, and the resulting supernatant was frozen at −70 °C.

Enrichment of Ubiquitinated Proteins—1.5 mg of a mouse monoclonal antibody directed against mono- and polyubiquitinated proteins (clone FK2, Enzo Life Sciences) was added to the lysate of pooled, labeled cells. After 2 h of incubation on ice, 400 μl of protein G-Sepharose beads that had been washed and equilibrated in lysis buffer were added, and the resulting mixture was incubated at 4 °C for 2 h with continuous mixing. The beads were then collected in a disposable column (Bio-Rad) and washed with 20 column volumes of lysis buffer containing MG132 and iodoacetamide as above. Bound material was then eluted in 250-μl fractions using a solution of 20 mM sodium phosphate, pH 7.2, 300 mM NaCl, 8 M urea containing protease inhibitors, MG132, and iodoacetamide as above (IMAC load buffer).

Protein-containing fractions were pooled and then incubated for 60 min at room temperature with 200 μl of TALON Superflow resin (Clontech) that had been equilibrated with IMAC load buffer. The TALON resin was collected in a disposable column and then washed with 20 column volumes of IMAC load buffer. Bound material was eluted in 100-μl fractions with a solution of IMAC load buffer containing 50 mM EDTA.

Aliquots of the resulting fractions were separated by SDS-PAGE, and those containing His_6-tagged proteins were identified on Western blots probed with a mouse anti-polyhistidine-horseradish peroxidase conjugate (Santa Cruz Biotechnology). Fractions containing the highest level of polyhistidine reactivity were selected for further analysis. Proteins were separated by SDS-PAGE and visualized with SimplyBlue SafeStain (Invitrogen).

Ubiquitinated Protein Enrichment and Analysis—The SDS-PAGE lane was excised and divided into 24–29 equal fractions of ~1.5-mm height. These bands were cut into ~1-mm cubes, and proteins were reduced with DTT, alkylated with iodoacetamide, and digested with trypsin (Promega, Madison, WI) using the ProGest Investigator in-gel digestion robot (Digilab, Holliston, MA) running the standard long trypsin digestion method. Recovered peptides were dried by SpeedVac and resolubilized in 6 μl of 0.1% TFA for LC-MS analysis.

A 5-μl sample was loaded onto a 15-cm × 75-μm column packed in-house with Vydac C18TP 5 μm 300 Å resin. Using a two-column switching system, the loading column was washed with 2% CH_3CN, 0.1% formic acid, 0.001% heptafluorobutyric acid for 90 min at 500 nl/min, followed by elution with a four phase linear gradient: 2–5% B over 2 min, 5–22% B over 38 min, 22–33% B over 10 min, 33–60% B over 10 min, with A = water with 0.1% formic acid and B = CH_3CN with 0.1% formic acid delivered by an Eksigent nanoLC-1D$^+$ (Dublin, CA) at 400 nl/min. Nanospray was performed using a NewObjective (Woburn, MA) source with peptides refocused in a 5-cm packed tip, pulled and packed in-house.

LC-MS analyses were performed using an LTQ-Orbitrap XL operated under Xcalibur 2.4 SP1 (ThermoFisher, San Jose, CA). A survey scan of 400–2000 m/z was performed in the Orbitrap at 60,000 resolution with AGC target of 1×10^6 and 500-ms injection time followed by five data-dependent MS^2 scans performed in the LTQ linear ion trap with one microscan, 100 ms of injection time, and 10,000 AGC. Dynamic exclusion was enabled, with repeat count of 1, exclusion duration of 30 s with exclusion list of 500. Ions of charge state one were rejected for ms/ms.

Ubiquitinated Peptide Enrichment and Analysis—SILAC-labeled HeLa TREx cell pellets were sent on dry ice to Cell Signaling Technology for UbiScan® analysis (K-GG peptide immunoprecipitation and LC-MS/MS) using the ubiquitin branch antibody (antibody 3925). Peptide preparation and immunoprecipitation were performed essentially as described (23). Briefly, cell pellets were brought to 10 ml each with urea lysis buffer, sonicated at 15 W output once for 25 s and twice for 15 s, and centrifuged 15 min at 20,000 × *g* to remove insoluble material. The resulting "cleared" protein extracts were reduced and carboxamidomethylated. Proteins were digested overnight with trypsin. Peptides were separated from nonpeptide material by solid phase extraction with Sep-Pak C18 cartridges. Lyophilized peptides were redissolved, and ubiquitinated peptides were isolated using slurries of the immobilized ubiquitin branch antibody. Peptides were eluted from antibody resin into a total volume of 100 μl in 0.15% TFA. Eluted peptides were concentrated with PerfectPure C18 tips immediately prior to LC-MS analysis. Peptides were loaded directly onto a 10-cm × 75-μm PicoFrit capillary column packed with Magic C18 AQ reversed phase resin. The column was developed with either a 45- or 100-min linear gradient of acetonitrile in 0.125% formic acid delivered at 280 nl/min. Tandem mass spectra were collected with an LTQ-Orbitrap hybrid mass spectrometer in profile mode, using a top 6 method, a dynamic exclusion repeat count of 1, and a repeat duration of 30 s. MS spectra were collected in the Orbitrap component of the mass spectrometer, and MS/MS spectra were collected in the LTQ.

Data Analysis—All quantitative SILAC analyses were performed using Elucidator, version 3.3.0.1.SP3_CRE52.21 (Rosetta Biosoftware, Seattle, WA). Retention time shifts for each SILAC pair were limited to 0.2 min, and mass accuracy of 5 ppm was required. Database searching was performed against the IPI human database version 3.52 concatenated with the reversed version of that database using both Mascot and Sage-N Sequest search engines. Search settings required 20-ppm peptide mass accuracy and 0.5-Da fragment ion tolerance and allowed two missed cleavages. Carbamidomethyl cysteine and the appropriate heavy SILAC residue masses (+6.020 Da or +8.014 Da for Lys and +6.020 Da or +10.008 Da for Arg) were included as static modifications, and methionine oxidation and diglycine modification of lysine were allowed as dynamic modifications as appropriate. Maximum observed false positive rates of 1% were used to annotate peptides and proteins using the Peptide and Protein Teller scripts within Elucidator. Note that contrary to the case when identifying phosphorylation sites, nearly all identified ubiquitinated peptides contain a single internal lysine residue, so there is no ambiguity in assignment of the ubiquitination sites necessitating additional analysis or validation.

In Vitro Ubiquitination Assays—Reaction mixtures containing 900 ng of UBE1 (produced at Amgen), 500 ng of UBCH5B (Lifesensors), GST-HRD1 lysate (Mesoscale Discovery), 72 μM ubiquitin (Mesoscale Discovery) or methylated ubiquitin (Boston Biochem), and 500 ng of GST-ATP6AP1 (Abnova) were

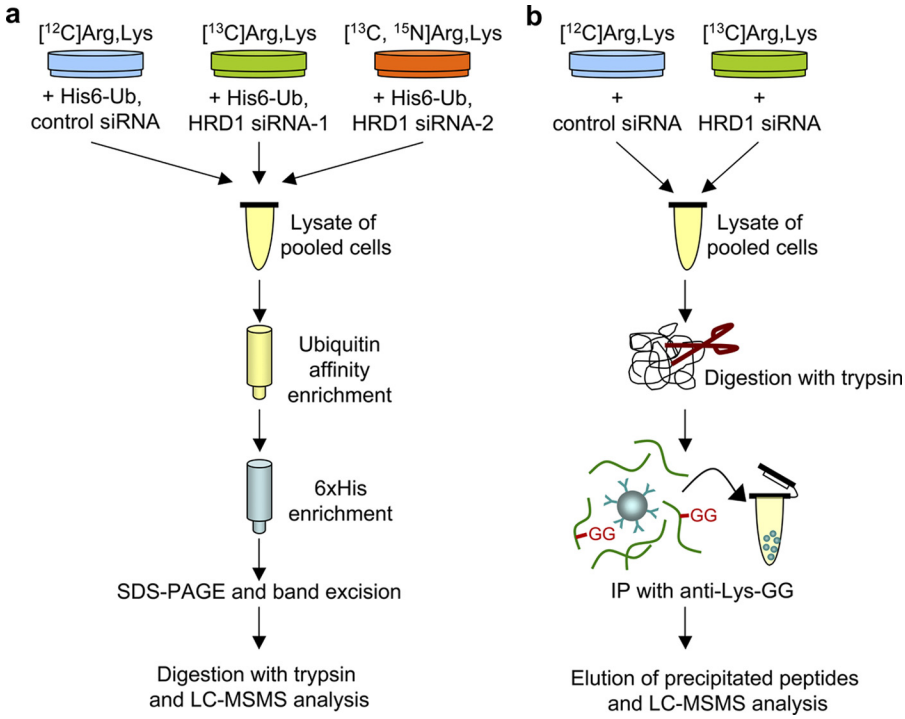

FIGURE 1. **Enrichment strategies for ubiquitinated proteins (*a*) and peptides (*b*).**

incubated in buffer containing 8 mM ATP, 2 mM DTT, 50 mM HEPES, pH 7.5, 100 mM NaCl, and 5 mM $MgCl_2$ in a total volume of 20 μl for 60 min at 30 °C. The reactions were then stopped with LDS sample buffer and reducing agent (Invitrogen) per the manufacturer's recommendations. The proteins were resolved by SDS-PAGE. Western blots were probed with mouse monoclonal antibody to ATP6AP1 (Santa Cruz Biotechnology) diluted 1:400 followed by a goat anti-mouse Alexa 680 conjugate (Licor) diluted 1:10,000 and visualized on a Licor Odyssey instrument.

RESULTS

To identify HRD1 substrates, we first established a method to enrich, identify, and quantify ubiquitinated proteins. Proteins extracted from HeLa TREx cells expressing His_6-tagged ubiquitin and grown in light or heavy SILAC medium, mixed at the point of harvest, were enriched for ubiquitinated proteins through a two-stage process. Immunoaffinity enrichment of all ubiquitinated proteins was performed as the first step, with eluting proteins further enriched through an IMAC chemical affinity step specific for the His_6-tagged ubiquitin. We found that use of the two orthogonal enrichment strategies led to maximum specificity of the method for ubiquitinated proteins. Proteins eluting from the IMAC enrichment were separated by SDS-PAGE and fractionated by slicing the gel lane into bands, with the proteins in the individual bands separately digested and analyzed by LC-MS/MS.

The specificity of this method was validated using cells expressing HA-tagged ubiquitin as a negative control and comparing with cells expressing His_6-tagged ubiquitin with quantitation by SILAC (supplemental Fig. S1). In this experiment, ubiquitinated proteins derived from the His_6-ubiquitin-expressing cells (heavy SILAC condition) are enriched compared with those derived from HA-ubiquitin-expressing cells (light), whereas nonubiquitinated background proteins are expected to appear at a 1:1 H:L ratio. Several peptides derived from ubiquitin itself were identified and quantified in this study, and they were found to be enriched in the heavy form, as expected (supplemental Fig. S2*a*). Many other proteins were observed as well, nearly all of which possessed a similar H:L ratio to ubiquitin itself (supplemental Fig. 2*b*). Quantitative analysis of these data using Elucidator revealed that the H:L ratio of the entire population of identified proteins is shifted to center around the ubiquitin H:L ratio (supplemental Fig. S3), validating the specificity of our two-step enrichment strategy and allowing for the assertion that essentially all proteins identified through this enrichment strategy are, in fact, ubiquitinated.

We applied our validated method to the task of identifying HRD1 substrates through the use of HRD1-specific siRNA technology. A three-way SILAC study was performed, comparing cells treated with control siRNA to cells treated with two different HRD1-specific siRNAs (Fig. 1*a*). We hypothesize that HRD1 substrates will have decreased ubiquitination levels and will be less abundant in our processed sample in cells with decreased HRD1 levels (both heavy SILAC conditions). 461 proteins were identified and quantified in this study (supplemental Tables S1 and S2). Most were quantitatively unaffected by the HRD1 knockdown, as expected (supplemental Fig. S4). However, the levels of a fraction of these ubiquitinated proteins were decreased with HRD1 knockdown, making them candidate HRD1 substrates (Table 1). For inclusion in this table, we required a decrease of 35% or more ($\log_2$ (ratio of Hrd1 siRNA/control) ≤ -0.43) in the levels of these proteins after our ubiquitination-based enrichment in the presence of at least one Hrd1 siRNA as compared with the control, some decrease with

TABLE 1

Candidate HRD1 substrates identified by protein level enrichment

Log_2(SILAC ratio of HRD1 siRNA/control) for each siRNA are reported. Transmembrane, lumenal, and secreted proteins (identified by database annotation) are indicated with bold italic type. Proteins with at least 35% reduction in signal with one HRD1-specific siRNA (−0.43 log_2 (ratio)), reduction in signal with both siRNAs (negative log_2(ratio)), and an average reduction at least one standard deviation below the median of all proteins detected are included.

Gene symbol	Protein description	siRNA 1	siRNA 2
ACSL3	***Long-chain-fatty-acid–CoA ligase 3***	−0.44	−0.16
ATP1A1	***Sodium/potassium-transporting ATPa***	−0.46	−0.26
ATP6AP1	***V-type proton ATPase subunit S1***	−1.19	−0.78
CD151	***CD151***	−0.51	−0.21
CD44	***CD44***	−0.78	−0.51
EPHA2	***ephrin receptor EphA2***	−0.61	−0.50
HLA-A	***HLA class I histocompatibility antigen, A-34 α***	−0.60	−0.20
HLA-A	***HLA class I histocompatibility antigen, A-2 α chain***	−0.67	−0.14
IFI44	Interferon-induced protein 44	−0.74	−0.24
IFITM2	***Interferon-induced transmembrane protein 2***	−0.55	−0.25
ITGA3	***Integrin α3***	−1.06	−0.01
ITGA6	***Integrinα6***	−0.65	−0.54
KCNN4	***Intermediate conductance calcium-activated potassium channel protein 4***	−0.63	−0.21
L1CAM	***Neural cell adhesion molecule L1***	−0.53	−0.12
LDHB	L-lactate dehydrogenase B chain	−4.27	−1.13
MYOF	***Myoferlin***	−0.75	−0.51
NFKB2	NF-κB p100 subunit	−0.38	−0.69
PPP1R15B	Protein phosphatase 1 regulatory subunit 15B	−0.76	−0.37
RNF31	RING finger protein 31	−0.56	−0.60
SLC12A3	***Solute carrier family 12 member 3***	−1.18	−0.62
SLC2A3	***Solute carrier family 2, facilitated glucose transporter member 3***	−0.46	−0.56
SLC30A1	***Zinc transporter 1***	−0.51	−0.32
SLC39A10	***Zinc transporter ZIP10***	−0.63	−0.37
SLC4A7	***Solute carrier family 4 sodium bicarbonate cotransporter member 7***	−0.20	−0.70
SLC7A2	***Low affinity cationic amino acid transporter 2***	−0.63	−0.28
SLC7A5	***Large neutral amino acids transporter small subunit 1***	−0.34	−0.48
STOM	***Erythrocyte band 7 integral membrane protein***	−0.50	−0.56
TNS4	Tensin-4	−0.64	−0.30
ZC3HAV1	Zinc finger CCCH-type antiviral protein 1	−0.32	−0.43

both Hrd1 siRNAs, and an average reduction at least one standard deviation below the median of all proteins detected. Note that, consistent with the known biology of HRD1 and its involvement in the ERAD process, nearly all of the identified candidate substrates are transmembrane proteins, lending credence to the validity of our findings.

As a parallel approach, we pursued a second strategy toward the same goal of HRD1 substrate identification, but at the ubiquitinated peptide level (Fig. 1*b*). Tryptic digestion of ubiquitinated proteins produces a peptide from the substrate protein with a missed cleavage at the ubiquitinated lysine. This lysine also retains the two C-terminal glycine residues from the ubiquitin protein attached to its side chain ϵ-amino group through an isopeptide linkage. This non-native K-GG motif is easily identified by LC-MS/MS as a 114-Da nominal mass shift localized to an internal lysine residue (11). The ubiquitin branch antibody (Cell Signaling Technology antibody 3925) has been produced to recognize and specifically immunoprecipitate peptides containing this K-GG motif.

Again using SILAC for quantitative comparison of cells with and without HRD1 siRNA, protein extracts were made and digested with trypsin. Peptides containing the K-GG ubiquitination motif were enriched through immunoprecipitation with the ubiquitin branch antibody. These peptides were eluted and analyzed by LC-MS/MS, and relative changes with and without HRD1 siRNA were quantified using Elucidator. Three different siRNAs were used to knock down HRD1 expression in parallel experiments to allow detection of single siRNA-specific events (supplemental Fig. S5). This study resulted in identification and quantification of more than 1800 ubiquitinated peptides from over 900 proteins (supplemental Tables S3 and S4). As expected, most ubiquitination sites were quantitatively unaffected by the presence or absence of HRD1, exhibiting a H:L ratio near 1:1 (supplemental Fig. S6). A fraction of these peptides were, however, quantitatively reduced in samples treated with HRD1-specific siRNA, making them candidate HRD1 substrates (Table 2; prerequisites for inclusion similar to those for Table 1; see table legend for details). Some responsive ubiquitination sites, such as those on phosphatidylinositol-4-phosphate 5-kinase type-1 α (PIP5K1A) and flightless 1 homolog (FLII), clearly do exhibit siRNA-specific effects (supplemental Table S3), but most have reproducible quantitative results across all three siRNAs used, consistent with ubiquitination by HRD1. As with our protein level approach, transmembrane proteins are again highly represented among the candidate HRD1 substrates.

Assessment of qualitative and quantitative reproducibility of this study was gained by replicating the study with HRD1 siRNA 1, with the proteasome inhibitor MG132 treatment as in our previous studies, and also without MG132 treatment. This allowed us both to determine whether observed effects were MG132-dependent and to explore the fate of the HRD1 substrate candidates after their ubiquitination. More than 400 ubiquitinated peptides were identified and quantified in this study, with the lower number caused by both the use of a shorter LC-MS gradient and the analysis of two rather than three independent samples in parallel. Both qualitatively and quantitatively, the results of this study were consistent with the previously described experiment (supplemental Fig. S7), with similar effects of HRD1 knockdown observed for candidate substrates both with and without proteasome inhibition. Looking at peptides derived from the ubiquitin protein itself, the

TABLE 2

Candidate HRD1 substrates identified by K-GG peptide immunoprecipitation

Log_2(SILAC ratio of HRD1 siRNA/control) for each siRNA are reported. Transmembrane, lumenal, and secreted proteins (identified by database annotation) are indicated with bold italic type. Ubiquitinated peptides with at least 35% reduction in signal with one HRD1-specific siRNA (−0.43 log_2 ratio), reduction in signal with all three siRNAs (negative log_2(ratio)), and an average reduction at least one standard deviation below the median of all proteins detected are included. Diglycine-modified lysine residues are followed by asterisks.

Symbol	Protein description	Peptide sequence	Ubiquitin site	siRNA 1	siRNA 2	siRNA 3
ABCC3	***Multidrug resistance-associated protein 3***	LYAWEPSFLK*QVEGIR	K512	−0.20	−0.06	−0.88
		VQVTEAK*ADGALTQEEK	K938	−1.34	−0.34	−1.21
ABCC4	***Multidrug resistance-associated protein 4***	MVQQLGK*AEAAALTETAK	K1278	−0.57	−0.83	−1.12
		GTYTEFLK*SGIDFGSLLK	K622	−0.64	−0.44	−0.81
ACP2	***Lysosomal acid phosphatase***	LLK*FPLGPCPR	K153	−0.23	−0.01	−0.79
ADAM9	***ADAM9***	SQTYESDGK*NQANPSR	K741	−0.30	−0.40	−1.14
		SQTYESDGK*NQANPSRQPGSVPR	K741	−0.15	−0.36	−1.13
ADCY9	***Adenylate cyclase type 9***	LTNSQTSLCEILQEK*GR	K699	−0.06	−0.72	−0.61
AES	N-terminal enhancer of split	HSGSSHLPQQLK*FTTSDSCDR	K19	−0.78	−0.16	−0.38
AHR	Aryl hydrocarbon receptor	NSDLYSIMK*NLGIDFEDIR	K544	−0.39	−0.44	−0.98
		HMQNEK*FFR	K560	−0.42	−0.39	−0.99
		SFFDVALK*SSPTER	K88	−0.00	−0.32	−0.90
AMOTL2	Angiomotin-like protein 2	LCPQPSK*GEELPTYEEAK	K100	−0.74	−0.68	−2.08
ANO10	***Anoctamin-10***	FALK*YQPIDSIR	K193	−0.46	−0.36	−0.52
APLP2	***Amyloid-like protein 2***	HLNK*MQNHGYENPTYK	K744	−0.53	−0.53	−0.29
ASF1B	Histone chaperone ASF1B	ENPPMK*PDFSQLQR	K129	−0.32	−0.15	−0.46
ATP1B3	***30-kDa protein***	FLK*PYTLEEQK	K115	−0.30	−0.33	−0.49
ATP6AP1	***V-type proton ATPase subunit S1***	ELK*LNASLPALLLIR	K168	−0.95	−0.80	−0.73
		EVLTGNDEVIGQVLSTLK*SEDVPYTAALTAVRPSR	K211	−0.80	−0.58	−0.76
AXL	***AXL receptor tyrosine kinase***	FMADIASGMEYLSTK*R	K666	−0.21	−0.46	−0.52
		LK*QPADCLDGLYALMSR	K769	−0.94	−0.50	−0.50
BCAT1	BCAT(c)	CILDLAHQWGEFK*VSER	K305	−0.49	−0.08	−0.78
BHLHE40	Class B basic helix-loop-helix protein 2	DLK*SSQLVTHLHR	K167	−0.55	−0.31	−0.43
		GSEGPGK*NCVPVIQR	K217	−0.46	−0.31	−0.30
		SEQPCFK*SDHGR	K262	−0.51	−0.43	−0.46
C15orf24	***UPF0480 protein C15orf24***	LPYPLQMK*SSGPPSYFIK	K141	−1.06	−0.34	−0.19
CALM3	Calmodulin	EAFSLFDKDGDGTITTK*ELGTVmR	K31	−0.53	−0.53	−0.11
CCND1	G1/S-specific cyclin-D1	AMLK*AEETCAPSVSYFK	K33	−0.82	−0.45	−0.70
CD44	***CD44***	KPSGLNGEASK*SQEMVHLVNK	K705	−0.53	−0.53	−0.55
CD46	***CD46***	K*GTYLTDETHR	K375	−0.48	−0.80	−0.24
CD46	***CD46 isoform B***	KGK*ADGGAEYATYQTK	K377	−0.62	−0.59	−0.16
CDA	Cytidine deaminase	IFK*GCNIENACYPLGICAER	K51	−0.40	−0.21	−0.76
CDK11B	Cyclin-dependent kinase 11B	ISAEDGLK*HEYFR	K719	−0.57	−0.03	−0.37
CEP164	Centrosomal protein of 164 kDa	LPSSVAQTVDDFLLEK*WR	K1359	−0.54	−0.45	−0.39
CRTAP	***Cartilage-associated protein***	LNDLK*NAAPCAVSYLLFDQNDK	K312	−1.26	−0.70	−1.18
CSPG4	***Chondroitin sulfate proteoglycan 4***	HDVQVLTAK*PR	K2263	−0.99	−0.31	−1.16
CTPS	CTP synthase 1	LSHYLQK*GCR	K557	−0.68	−0.07	−0.15
CYB561	***Cytochrome b_{561}***	RPSQAEEQALSMDFK*TLTEGDSPGSQ	K240	−0.03	−0.59	−0.24
CYP1B1	***Cytochrome P450 1B1***	NFSNFILDK*FLR	K275	−0.29	−0.28	−0.68
DAB2	Disabled homolog 2	TGK*QEAQAGPWPFSSSQTQPAVR	K356	−0.45	−0.38	−0.58
DAG1	***Dystroglycan***	GVPIIFADELDDSK*PPPSSSmPLILQEEK	K808	−0.31	−0.24	−1.01
DCTN1	Dynactin subunit 1	TSPAAK*SPSAQLMEQVAQLK	K1179	−0.63	−0.11	−0.51
DDX12	DEAD/H box protein 12	ALVENLCMK*AVNQSIGR	K858	−0.14	−0.30	−0.55
DIO2	***Type II iodothyronine deiodinase***	CVWK*SFLLDAYK	K65	−0.74	−0.43	−0.48
DPYD	Dihydropyrimidine dehydrogenase	QAVQIPFFAK*LTPNVTDIVSIAR	K709	−0.48	−0.06	−0.54
DUSP1	Dual specificity protein phosphatase 1	LDEAFEFVK*QR	K289	−0.70	−0.03	−0.19
EEF1AL3	Putative elongation factor 1α-like 3	STTTGHLIYK*CGGIDKR	K30	−0.77	−0.49	−0.42
ERCC6	DNA excision repair protein ERCC-6	EILQEFESK*LSASQSCVFR	K1457	−0.41	−0.58	−0.26
EXT2	***exostosin 2***	QGYDVSIPVYSPLSAEVDLPEK*GPGPR	K245	−0.51	−0.44	−0.50
F3	***Tissue factor***	AGVGQSWK*ENSPLNVS	K287	−0.84	−1.18	−0.84
FANCG	Fanconi anemia group G protein	DTYFHLLQTLK*R	K559	−1.03	−0.16	−0.06
FASN	Fatty acid synthase	VFTTVGSAEK*R	K1704	−0.50	−0.25	−0.19
FOLR1	***Folate receptor α***	FNWNHCGEMAPACK*R	K97	−0.67	−0.34	−1.63
GANAB	***Neutral α-glucosidase AB***	LK*VTEGGEPYR	k269	−0.31	−0.01	−0.69
		TLFGK*MMDYLQGSGETPQTDVR	K337	−0.43	−0.29	−0.82
GGCX	***γ-Glutamyl carboxylase isoform 2***	LQQLLPLK*AAPQPSVSCVYK	K334	−0.11	−0.07	−0.69
GNB2	G protein subunit β2	LLLAGYDDFNCNIWDAmK*GDR	K301	−0.50	−0.18	−0.19
GPRC5A	***Retinoic acid-induced protein 3***	NPMDYPVEDAFCK*PQLVK	K285	−1.06	−0.77	−0.58
HERC5	hect domain and RLD 5	DYVSK*YINYIFNDSVK	K867	−0.55	−0.25	−0.53
HLA-A	***MHC class I antigen A*2***	YLENGK*ETLQR	K200	−0.64	−0.14	−0.36
		GGSYSQAASSDSAQGSDVSLTACK*V	K364	−0.50	−0.36	−0.07
HLA-C	***MHC class I antigen Cw*15***	GGSCSQAASSNSAQGSDESLIACK*A	K365	−0.51	−0.32	−0.07
HNRNPM	Heterogeneous nuclear ribonucleoprotein M	INEILSNALK*R	K381	−0.82	−0.25	−0.52
		RGEIIAK*QGGGGGGGSVPGIER	K388	−0.64	−0.23	−0.03
HSPB1	Heat shock protein β1	TK*DGVVEITGK	K114	−0.45	−0.15	−0.61
IGF1R	***Insulin-like growth factor 1 receptor***	KGGK*GLLPVR	K1171	−0.51	−0.34	−0.23
IL7R	***Interleukin-7 receptor subunit α***	DEVEGFLQDTFPQQLEESEK*QR	K337	−0.72	−0.39	−0.83
IRAK2	IL-1 receptor-associated kinase-like 2	SPVYLK*DLLLSDIPSSTASLCSR	K425	−0.75	−0.21	−0.36
ITGA3	***Integrin α3, isoform α3A***	AEMK*SQPSETERLTDDY	K1038	−0.95	−0.51	−0.96
ITGA6	***Integrin α6***	QWITK*WNENESYS	K1122	−0.37	−0.21	−0.49
ITGAV	***Integrin αV***	ASGDFQTTK*LNGFEVFAR	K360	−0.52	−0.25	−0.63
ITGB1	***Integrin β1***	WDTGENPIYK*SAVTTVVNPK	K784	−0.44	−0.00	−0.55
ITGB4	***Integrin β4***	AFHDLK*VAPGYYTLTADQDAR	K915	−1.01	−0.98	−0.96
LAPTM4A	***Lysosomal-associated TM protein 4A***	MPEK*EPPPPYLPA	K224	−0.52	−0.37	−0.67
LGALS3BP	***Galectin-3-binding protein***	SDLAVPSELALLK*AVDTWSWGER	K323	−0.70	−0.50	−0.28
LMBRD2	***LMBR1 domain-containing protein 2***	KCPTEYQEK*MGR	K282	−0.78	−0.56	−0.06
MAGEA1	Melanoma-associated antigen 1	AREPVTK*AEMLESVIK	K125	−1.19	−0.90	−0.57
MCAM	***Cell surface glycoprotein MUC18***	APGDQGEK*YIDLR	K640	−0.56	−0.40	−0.57
MED25	Mediator complex subunit 25	LLFEK*AAPPALLEPLQPPTDVSQDPR	K197	−0.32	−0.58	−0.21
MGRN1	Probable E3 ubiquitin-protein ligase MGRN1	SPSLQSETVHYK*R	K164	−0.37	−0.62	−0.06
NDFIP2	***NEDD4 family-interacting protein 2***	AK*AAAMAAAAAETSQR	K193	−0.50	−0.42	−0.30

TABLE 2—*continued*

Symbol	Protein description	Peptide sequence	Ubiquitin site	siRNA 1	siRNA 2	siRNA 3
NUDT21	CPSF 25-kDa subunit	YIQQTK*PLTLER	K29	−0.14	−0.48	−0.31
OLR1	***Oxidized low density lipoprotein receptor 1***	IQTVK*DQPDEK	K12	−0.79	−0.68	−1.13
PCBP1	Poly(rC)-binding protein 1	QMSGAQIK*IANPVEGSSGR	K314	−0.73	−0.67	−0.43
PFN1	Profilin-1	EGVHGGLINK*K	K126	−0.19	−0.04	−1.08
PLD2	Phospholipase D2	TVLNK*VGDEIVDR	K656	−0.51	−0.30	−0.39
PNPLA2	***Patatin-like phospholipase protein 2***	NNLSLGDALAK*WEECQR	K435	−0.30	−0.11	−0.60
PODXL	***PODXL protein***	KVVSLNGELGDSWIVPLDNLTK*DDLDEEEDTHL	K547	−0.61	−0.48	−0.56
POLR2B	DNA-directed RNA pol. II subunit RPB2	HAIYDK*LDDDGLIAPGVR	K847	−0.49	−0.19	−0.15
PPAP2B	***Lipid phosphate phosphohydrolase 3***	AIVPESK*NGGSPALNNNPR	K15	−0.33	−0.60	−0.78
PSMC3	26 S protease regulatory subunit 6A	ATFLK*LAGPQLVQmFIGDGAK	K250	−0.62	−0.10	−0.29
PTBP1	Polypyrimidine tract-binding protein 1	VSFSK*STI	K528	−0.33	−0.41	−0.45
PTPRJ	***Protein-tyrosine phosphatase eta***	VENFEAYFK*K	K1031	−0.55	−0.24	−0.52
PTRF	Polymerase I and transcript release factor	QAEMEGAVQSIQGELSK*LGK	K95	−0.33	−0.29	−0.75
		LGK*AHATTSNTVSK	K98	−0.78	−0.01	−0.23
RAB10	Ras-related protein Rab-10	SFENISK*WLR	K102	−0.28	−0.04	−0.66
RAB34	Ras-related protein Rab-34	VAALTFEANVLAELEK*SGAR	K227	−0.29	−0.06	−0.93
RPL10	60 S ribosomal protein L10	FNADEFEDMVAEK*R	K188	−0.44	−0.26	−0.26
RPL18	60 S ribosomal protein L18	AGGK*ILTFDQLALDSPK	K119	−0.44	−0.38	−0.40
RPN2	***Ribophorin II***	LEHAK*SVASR	K311	−0.71	−0.14	−0.23
SCARA3	***Scavenger receptor class A member 3***	TGEAVK*NIQATLGASSQR	K277	−0.46	−0.15	−0.20
SETX	Probable helicase senataxin	K*GAEGIEEHTRPR	K1133	−0.45	−0.19	−0.30
		ISPASYNK*EESEQMGK	K621	−0.41	−0.44	−0.41
		ISPASYNKEESEQMGK*TSR	K629	−0.43	−0.40	−0.36
SKIV2L	Helicase SKI2W	AHEQALAELTK*R	K791	−0.59	−0.39	−0.36
SLC12A3	***Solute carrier family 12 member 3***	MMQAHINPVFDPAEDGK*EASAR	K801	−0.48	−0.91	−0.78
		ALVK*EEQATTIFQSEQGKK	K814	−0.40	−0.92	−1.21
SLC16A1	***Monocarboxylate transporter 1***	EEETSIDVAGK*PNEVTK	K473	−0.51	−0.38	−0.40
SLC1A5	***Neutral amino acid transporter B(0)***	CVEENNGVAK*HISR	K372	−0.31	−0.25	−0.46
SLC20A1	***Sodium-dependent phosphate transporter 1***	TVSFK*LGDLEEAPER	K320	−0.36	−0.40	−0.52
SLC27A3	Long chain fatty acid transport protein 3	YLVNQPPSK*AER	K436	−0.14	−0.21	−0.60
SLC2A1	***Glucose transporter type 1***	QGGASQSDK*TPEELFHPLGADSQV	K477	−0.23	−0.19	−0.46
SLC2A3	***Glucose transporter type 3***	SGK*DGVMEMNSIEPAKETTTNV	K477	−0.26	−0.45	−0.52
		SGKDGVMEMNSIEPAK*ETTTNV	K490	−0.29	−0.33	−0.68
SLC30A1	***Zinc transporter 1***	TQCALK*QCCGTLPQAPSGK	K444	−0.73	−0.41	−0.19
		NMPNK*QPESSL	K501	−0.49	−0.70	−0.46
SLC35B2	***PAPS transporter 1***	AVPVESPVQK*V	K431	−0.26	−0.38	−1.07
SLC35C2	***Solute carrier family 35 member C2***	ALK*GLGSSPDLELLLR	K331	−0.21	−0.30	−0.53
SLC3A2	***4F2 cell surface antigen heavy chain***	NGLVK*IK*VAEDEAEAAAAAK	K145,K147	−0.07	−0.59	−0.34
		IK*VAEDEAEAAAAAK	K147	−0.21	−0.50	−0.10
SLC43A2	***Solute carrier family 43 member 2***	SAK*EQVALQEGHK	K283	−0.93	−0.57	−0.11
SLC43A3	***Solute carrier family 43 member 3***	EETPGAGQK*QELR	K264	−0.28	−0.44	−0.25
		EFLSAKEETPGAGQK*QELR	K264	−0.26	−0.66	−0.23
SLC6A6	***Sodium- and chlorine-dependent taurine transporter***	DILK*PSPGK	K19	−0.06	−0.37	−0.63
		SPGTRPEDEAEGK*PPQR	K37	−0.28	−0.75	−0.98
SLC7A5	L-Amino acid transporter 1	ALAAPAAEEK*EEAR	K19	−0.15	−0.51	−0.31
		ALAAPAAEEK*EEAREK	K19	−0.19	−0.55	−0.24
		EK*MLAAK*SADGSAPAGEGEGVTLQR	K25, K30	−0.36	−0.78	−0.36
		mLAAK*SADGSAPAGEGEGVTLQR	K30	−0.16	−0.67	−0.28
		MLAAK*SADGSAPAGEGEGVTLQR	K30	−0.15	−0.62	−0.18
SLCO4A1	***SLC organic anion transporter 4A1***	GEASNPDFGK*TIR	K367	−0.67	−0.51	−0.51
SNAP23	Synaptosomal-associated protein 23	TITMLDEQK*EQLNR	K49	−0.33	−0.52	−0.42
SRP72	Calmodulin kinase II isoform	LTMAQLK*ISQGNISK	K383	−0.33	−0.45	−0.06
TARS	Threonyl-tRNA synthetase, cytoplasmic	AEHDSILAEK*AEK	K75	−2.39	−2.55	−1.64
TFRC	***Transferrin receptor protein 1***	QVDGDNSHVEMK*LAVDEEENADNNTK	K39	−0.20	−0.58	−0.29
TMEM106B	***Transmembrane protein 106B***	SLSHLPLHSSK*EDAYDGVTSENMR	K14	−0.26	−0.58	−0.52
TRERF1	Transcriptional-regulating factor 1	QLLSQK*PMEPPAPAIPSR	K188	−0.34	−0.26	−0.56
		DGLGLPVGSK*NLGQMDTSR	K72	−0.45	−0.19	−0.89
UNC13D	Unc-13 homolog D	LVIGK*LPAQLAWEALEQR	K714	−0.72	−0.15	−0.41
USP24	Putative uncharacterized protein USP24	MWNK*ELYVR	K1764	−0.06	−0.32	−0.71
USP5	Ubiquitin C-terminal hydrolase 5	ALIGK*GHPEFSTNR	K423	−0.34	−0.77	−0.20
VAMP7	***Vesicle-associated membrane protein 7***	GERLELLIDK*TENLVDSSVTFK	K160	−0.15	−0.52	−0.15
ZNF281	ZNF281	TTYQIENFAQAFGSQFK*SGSR	K840	−0.30	−0.33	−0.44

level of the ubiquitin K48-diglycine peptide is increased in the presence of MG132, as expected, because K48 linkages are associated with proteasome-targeted protein degradation. Also as expected, the ubiquitin K63-diglycine peptide is quantitatively unaffected by MG132 treatment.

Both the protein level and peptide level enrichment strategies yielded collections of candidate HRD1 substrates that contained striking numbers of transmembrane, lumenal, and secreted proteins, 76 and 56%, respectively (Tables 1 and 2), compared with 26 and 24%, respectively, for the total population of ubiquitinated proteins detected in the two enrichment approaches (supplemental Fig. S8). That both methods identified candidate HRD1 substrates highly enriched for potential ERAD targets, consistent with the known function of HRD1, provides further support for the validity of our two approaches.

Comparing the results obtained by both the protein level and peptide level analyses reveals that a surprising number of candidate substrate proteins were identified by both of these highly divergent strategies, with similar quantitative effects of each HRD1 siRNA (Fig. 2). This qualitative and quantitative overlap gives us a high degree of confidence in the results obtained by each method. Furthermore, HRD1 substrates identified by both methods can be considered validated, because two independent approaches have confirmed their sensitivity to HRD1, whereas proteins and sites of ubiquitination found by only one method are classified as candidate substrates until confirmation can be made by other means.

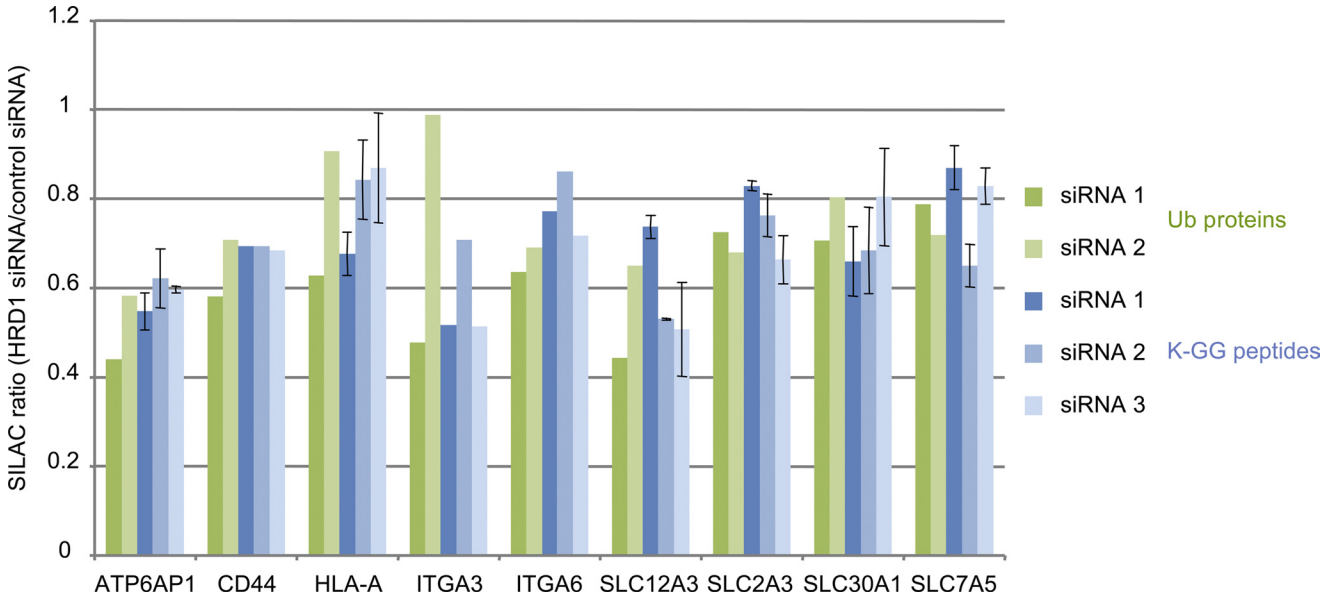

FIGURE 2. **Substrates for HRD1 identified both at protein level and at peptide level.** Although the two methods employed used vastly different strategies, the population of candidate substrates from each approach is highly overlapping, validating both methods. Representative HRD1 substrates are presented, with their quantitative response to HRD1 siRNAs both at the protein and peptide levels. The *error bars* represent one standard deviation of the values obtained in the peptide level experiment for proteins for which more than one ubiquitinated peptide was identified.

To test whether substrates identified by our proteomic studies could in fact be ubiquitinated by HRD1, we examined the ubiquitination of ATP6AP1 *in vitro* (Fig. 3). In a ubiquitination reaction with ATP6AP1, HRD1 generated a ladder of more slowly migrating species indicative of polyubiquitination of ATP6AP1. These species were not detected when HRD1 was omitted from the reaction, indicating that HRD1 is required for their generation. In reactions performed with methylated ubiquitin, which prevents elongation of ubiquitin chains, monoubiquitinated ATP6AP1 was still detected, but more slowly migrating species were eliminated, confirming that the ladder seen in the *second lane* of Fig. 3 is due to polyubiquitination of ATP6AP1. That HRD1 can promote ubiquitination of ATP6AP1 in a biochemical assay further confirms that our proteomic approaches identified *bona fide* HRD1 substrates.

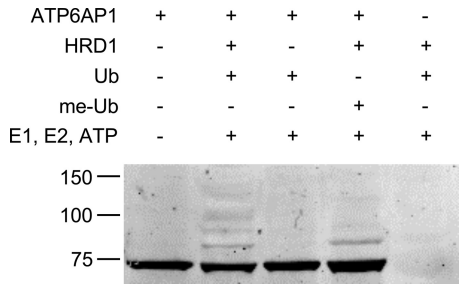

FIGURE 3. ***In vitro* ubiquitination of ATP6AP1 by HRD1.** ATP6AP1 was incubated with HRD1, ubiquitin (*Ub*) or methylated ubiquitin (*me-Ub*), and E1, E2 (UbCH5B), and ATP as indicated. The reactions were separated by SDS-PAGE, and ATP6AP1 species were detected on Western blots probed with a monoclonal antibody to ATP6AP1. Migration of molecular mass markers in kDa is indicated.

DISCUSSION

Striking among the substrates identified by both methods is the MHC class I molecule HLA. In a recent study of ERAD of HLA, depletion of HRD1 with siRNA impaired degradation of misfolded HLA, as did overexpression of a dominant negative form of HRD1 (24). In addition, HRD1 depletion reduced HLA ubiquitination in cells, and HRD1 coimmunoprecipitated with misfolded, but not properly folded, HLA. The identification of an independently validated HRD1 substrate in our study further confirms the power of our methods.

The role, if any, of the HRD1 substrates we have identified in rheumatoid arthritis of course remains to be elucidated. HRD1 overexpression in RA would be predicted to down-regulate cell surface HLA and hence class I antigen presentation. Mice lacking $CD8^+$ T cells, which recognize antigen presented by class I, develop disease normally in arthritis models (25). However, CD8+ Treg cells have been reported to suppress a mouse model of arthritis (26), suggesting that in the appropriate context, down-regulation of class I by overexpressed HRD1 might promote inflammation.

CD44 is a transmembrane glycoprotein with 17 different protein isoforms described in the UniProtKB database. CD44-deficient mice show increased disease in arthritis models (27), consistent with the hypothesis that HRD1-driven down-regulation of CD44 might contribute to RA. However, CD44 blocking antibodies reduce the severity of mouse arthritis models (24). Therefore, an understanding of the sites of HRD1 overexpression and knowledge of the functions of the CD44 isoforms expressed at those sites is needed before a disease role for HRD1-mediated ubiquitination of CD44 can be assigned.

Finally, both the protein level and peptide level enrichment studies identified multiple integrin chains as potential HRD1 substrates. Among these, integrins $\alpha 3$ and $\alpha 6$ were validated in both studies. Integrin $\alpha 6\beta 1$ has been shown to be expressed in fibroblast-like synoviocytes (28), the cell type in which HRD1 was originally shown to be overexpressed in RA. Integrin $\beta 1$ was a strong candidate substrate in the peptide level enrichment study (Table 2), whereas one of two siRNAs decreased its

signal in the protein level enrichment experiment (supplemental Table S1). Thus, it is possible that HRD1 down-regulates both chains of integrin $\alpha 6\beta 1$ in RA synoviocytes. This down-regulation could alter the adhesion or migratory behavior of synoviocytes and hence their invasion into cartilage in bone, contributing to disease. However, in all cases, demonstration that HRD1 overexpression reduces the cell surface expression, and function of the substrates we have identified awaits experimental confirmation.

In summary, we have established and utilized two approaches to identify substrates of the ubiquitin E3 ligase HRD1. Each approach is effective, and a similar population of ubiquitinated proteins has been discovered using each method, allowing confident identification of HRD1 substrates. These two strategies can be readily applied to interrogate the biology surrounding other E3 ligases and could be easily adapted to the study of other enzymes in the ubiquitin pathway as well as other ubiquitin-like molecules.

Acknowledgments—We thank Hao Chen for construction of tagged ubiquitin expression vectors, Roxanne Splett-Young for expert and patient bureaucratic navigation, and Jo Hulme and Duke Virca for support of this work.

REFERENCES

1. Acconcia, F., Sigismund, S., and Polo, S. (2009) *Exp. Cell Res.* **315,** 1610–1618
2. Chen, Z. J., and Sun, L. J. (2009) *Mol. Cell* **33,** 275–286
3. Pickart, C. M. (2004) *Cell* **116,** 181–190
4. Deshaies, R. J., and Joazeiro, C. A. (2009) *Annu. Rev. Biochem.* **78,** 399–434
5. Bays, N. W., Gardner, R. G., Seelig, L. P., Joazeiro, C. A., and Hampton, R. Y. (2001) *Nat. Cell Biol.* **3,** 24–29
6. Kaneko, M., Ishiguro, M., Niinuma, Y., Uesugi, M., and Nomura, Y. (2002) *FEBS Lett.* **532,** 147–152
7. Kikkert, M., Doolman, R., Dai, M., Avner, R., Hassink, G., van Voorden, S., Thanedar, S., Roitelman, J., Chau, V., and Wiertz, E. (2004) *J. Biol. Chem.* **279,** 3525–3534
8. Amano, T., Yamasaki, S., Yagishita, N., Tsuchimochi, K., Shin, H., Kawahara, K., Aratani, S., Fujita, H., Zhang, L., Ikeda, R., Fujii, R., Miura, N., Komiya, S., Nishioka, K., Maruyama, I., Fukamizu, A., and Nakajima, T. (2003) *Genes Dev.* **17,** 2436–2449
9. Toh, M. L., Marotte, H., Blond, J. L., Jhumka, U., Eljaafari, A., Mougin, B., and Miossec, P. (2006) *Arthritis Rheum.* **54,** 2109–2118
10. Gao, B., Calhoun, K., and Fang, D. (2006) *Arthritis Res. Ther.* **8,** R172
11. Toh, M. L., Gonzales, G., Koenders, M. I., Tournadre, A., Boyle, D., Lubberts, E., Zhou, Y., Firestein, G. S., van den Berg, W. B., and Miossec, P. (2010) *PLoS One* **5,** e13416
12. Peng, J., Schwartz, D., Elias, J. E., Thoreen, C. C., Cheng, D., Marsischky, G., Roelofs, J., Finley, D., and Gygi, S. P. (2003) *Nat. Biotechnol.* **21,** 921–926
13. Matsumoto, M., Hatakeyama, S., Oyamada, K., Oda, Y., Nishimura, T., and Nakayama, K. I. (2005) *Proteomics* **5,** 4145–4151
14. Vasilescu, J., Smith, J. C., Ethier, M., and Figeys, D. (2005) *J. Proteome Res.* **4,** 2192–2200
15. Mayor, T., Lipford, J. R., Graumann, J., Smith, G. T., and Deshaies, R. J. (2005) *Mol. Cell. Proteomics* **4,** 741–751
16. Seyfried, N. T., Xu, P., Duong, D. M., Cheng, D., Hanfelt, J., and Peng, J. (2008) *Anal. Chem.* **80,** 4161–4169
17. Xu, G., Paige, J. S., and Jaffrey, S. R. (2010) *Nat. Biotechnol.* **28,** 868–873
18. Kim, W., Bennett, E. J., Huttlin, E. L., Guo, A., Li, J., Possemato, A., Sowa, M. E., Rad, R., Rush, J., Comb, M. J., Harper, J. W., and Gygi, S. P. (2011) *Mol. Cell* 10.1016/j.molcel. 2011.08.025
19. Wagner, S. A., Beli, P., Weinert, B. T., Nielsen, M. L., Cox, J., Mann, M., and Choudhary, C. (2011) *Mol. Cell. Proteomics* 10.1074/mcp.M111.013284
20. Emanuele, M. J., Elia, A. E., Xu, Q., Thoma, C. R., Izhar, L., Leng, Y., Guo, A., Chen, Y. N., Rush, J., Hsu, P. W., Yen, H. C., and Elledge, S. J. (2011) *Cell* **10,** 459–474
21. Ong, S. E., Blagoev, B., Kratchmarova, I., Kristensen, D. B., Steen, H., Pandey, A., and Mann M. (2002) *Mol. Cell. Proteomics* **1,** 376–386
22. Lössner, C., Warnken, U., Pscherer, A., and Schnölzer, M. (2011) *Anal. Biochem.* **412,** 123–125
23. Rush, J., Moritz, A., Lee, K. A., Guo, A., Goss, V. L., Spek, E. J., Zhang, H., Zha, X. M., Polakiewicz, R. D., and Comb, M. J. (2005) *Nat. Biotechnol.* **23,** 94–101
24. Burr, M. L., Cano, F., Svobodova, S., Boyle, L. H., Boname, J. M., and Lehner, P. J. (2011) *Proc. Natl. Acad. Sci. U.S.A.* **108,** 2034–2039
25. Ehinger, M., Vestberg, M., Johansson, A. C., Johannesson, M., Svensson, A., and Holmdahl, R. (2001) *Immunology* **103,** 291–300
26. Notley, C. A., McCann, F. E., Inglis, J. J., and Williams, R. O. (2010) *Arthritis Rheum.* **62,** 171–178
27. Naor, D., Nedvetzki, S., Walmsley, M., Yayon, A., Turley, E. A., Golan, I., Caspi, D., Sebban, L. E., Zick, Y., Garin, T., Karussis, D., Assayag-Asherie, N., Raz, I., Weiss, L., Slavin, S., and Golan, I. (2007) *Ann. N.Y. Acad. Sci.* **1110,** 233–247
28. Pirilä, L., Aho, H., Roivainen, A., Konttinen, Y. T., Pelliniemi, L. J., and Heino, J. (2001) *J. Rheumatol.* **28,** 478–484